C. R. Mecanique 344 (2016) 251–266

Contents lists available at ScienceDirect

Comptes Rendus Mecanique

www.sciencedirect.com

Computational simulation of manufacturing processes

Lagrangian and arbitrary Lagrangian Eulerian simulations of complex roll-forming processes

Yanick Crutzen, Romain Boman, Luc Papeleux, Jean-Philippe Ponthot *

LTAS – Computational Mechanics, University of Liège, 9 allée de la Découverte, B-4000 Liège, Belgium

ARTICLE INFO

Article history:
Received 27 April 2015
Accepted after revision 25 November 2015
Available online 2 March 2016

Keywords:
Cold roll forming
Finite element method
ALE formalism
Springback

ABSTRACT

The Arbitrary Lagrangian Eulerian (ALE) formalism is a breakthrough technique in the numerical simulation of the continuous-type roll-forming process. In contrast to the classical Lagrangian approach, the ALE formalism can compute the hopefully stationary state for the entire mill length with definitely effortless set-up tasks thanks to a nearly-stationary mesh. In this paper, advantages of ALE and Lagrangian formalisms are extensively discussed for simulating such continuous-type processes. Through a highly complex industrial application, the ease of use of ALE modelling is illustrated with the in-house code METAFOR. ALE and Lagrangian results are in good agreement with each other.

1. Introduction

In the manufacturing industry, cold roll forming has achieved a renewed interest since high-yield-strength metals have been brought to the market. According to recent expectations, roll-formed sections will be even very common in the near future for automotive industry [1]. The primary reason is that it is a convenient way for forming materials with high mechanical strength circumventing limitations of the classical deep drawing process for such materials (e.g., limited press power, sheet tearing, large springback, limited formability, etc.). Besides, roll forming provides a high productivity and complex shaped cross-sections.

In cold roll forming, the material is fed into the mill as a flat pre-cut or continuous strip and is incrementally formed through successive roll stands until the desired cross-sectional shape is obtained. In a continuous forming method (also named post-cut method), the material is typically coiled and cut to length after roll forming. In most cases, the continuous forming method is adopted in the industry [2,3] since the pre-cut method exhibits a certain number of drawbacks. Contrary to the post-cut method, the pre-cut forming method requires a minimum product length: the product length should be at least equal to twice the inter-stand distance to ensure that the strip is engaged in a minimum of two stands at any time of the forming process (see Fig. 1). In addition, the end-flare defect is usually larger when pre-cut sheets are roll formed. Moreover, the forming tools are more prone to wear or even damage, especially due to the leading and trailing ends of the pre-cut strip that can hit the tooling. Designing a pre-cut mill requires thus extra care, resulting usually in a higher number

* Corresponding author. Tel.: +32 04 3669310.
E-mail addresses: Y.Crutzen@ulg.ac.be (Y. Crutzen), R.Boman@ulg.ac.be (R. Boman), L.Papeleux@ulg.ac.be (L. Papeleux), JP.Ponthot@ulg.ac.be (J.-P. Ponthot).
URL: http://www.ltas-mnl.ulg.ac.be (J.-P. Ponthot).

http://dx.doi.org/10.1016/j.crme.2016.02.005
1631-0721/

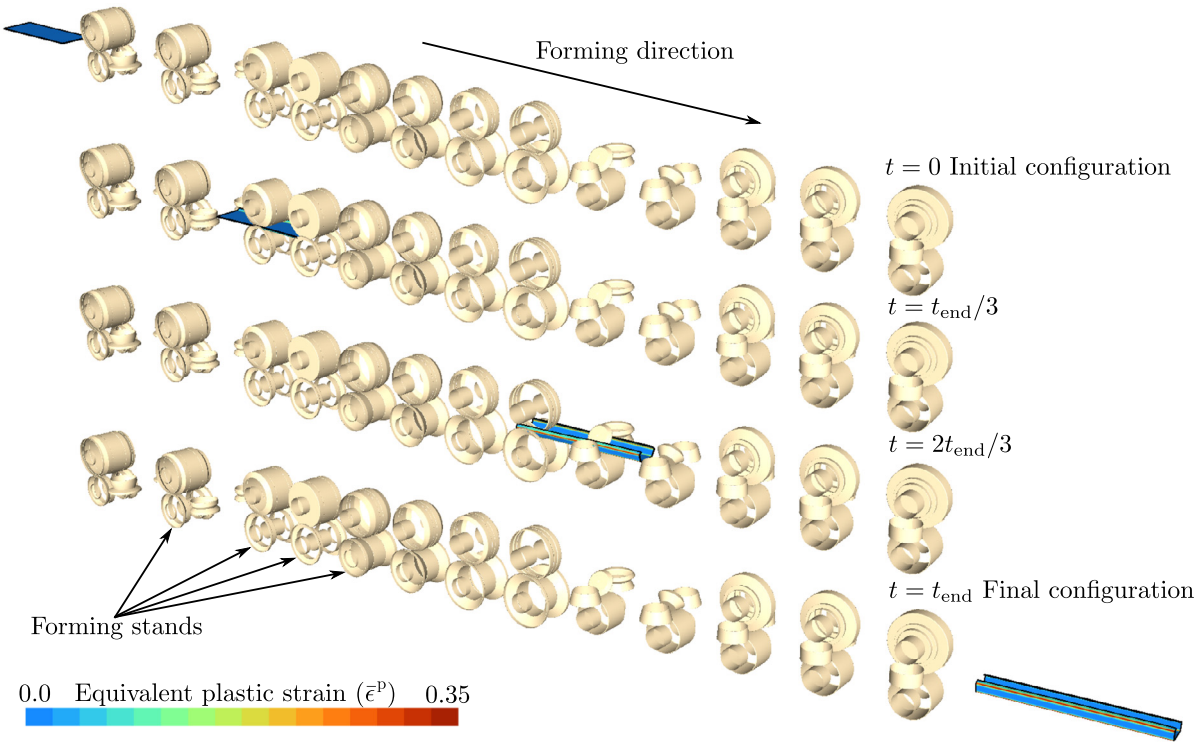

Fig. 1. Illustration of the progress of a Lagrangian roll forming simulation of a C-channel as proposed in [4] with the pre-cut method using METAFOR [5,6] (sheet length = 710 mm − inter-stand distance = 300 mm).

of forming stands and, in turn, in a possible higher investment cost. Finally, a distinct advantage of a post-cut mill is that several auxiliary operations such as punching, sweeping, welding, longitudinal bending, etc. can be gathered in-line to form a single complete unit, removing the need for handling cost.

Finite element analysis (FEA) is regarded in industry as an essential tool for the early design and optimization stages of a roll-forming mill. Complex deformations occur during the roll-forming process, involving possible shape defects on the final product such as longitudinal bow, oil canning, end-flare, etc. Hence, the designers' know-how based on empiricism or some simplified formulae [3] cannot be sufficient for ensuring the demanding quality of the product. In addition, the introduction of new high-strength materials into a relatively ancient forming process is a challenging task for the designers. In particular, mastering the larger springback experienced with the higher strength materials is by far not a straightforward operation, regarding the tight dimensional tolerances required for the roll-formed product. As a result, attempts to simulate the roll forming process by the finite element method are multiplying in the literature [7–23].

However, for such a problem, FEA generally remains incredibly time-consuming, thus limited, in the scientific literature, to some simple cases (exceptions can be found in [8–11,14]) and to the pre-cut forming method (exceptions can be found in [12,14]) and thereby does not fit very well in today's competitive industry. These numerical models rely on a Lagrangian kinematical description where the mesh follows the material's motion. In such Lagrangian models, an initially-flat pre-cut strip is formed in the successive forming stands (the progress of such a Lagrangian simulation can be seen in Fig. 1). This kind of formalism is not very well suited for simulating the continuous roll-forming process. Indeed, the modelled strip should be ideally longer than twice the length of the mill, resulting in costly and certainly not affordable numerical models. Consequently, in industrial practice, these difficulties hinder the intensive use of FEA in the design of roll-forming mills.

The application of the Arbitrary Lagrangian Eulerian (ALE) formalism to continuous roll-forming simulations as presented here is an effective alternative to the classical Lagrangian one (see Fig. 2). This approach definitely represents an original proposition on a market dominated by the Lagrangian kinematics. It does not follow the technology standards established especially by COPRA, the leader in software technology for roll-formed sections simulation, with its dedicated module COPRA FEA RF [24]. In contrast to the conventional Lagrangian approach, the ALE formalism, which consists in decoupling the motion of the material and the mesh, has the capability to compute the hopefully stationary state of the continuous process for the entire roll forming line at an acceptable response time by using a nearly-stationary mesh. In the particular case of roll forming, the mesh nodes are globally fixed in the forming direction but are free to move in transverse directions. Taking advantage from this approach, the mesh is only refined in the close neighbourhoods of the forming tools for accurate modelling of contact and bending. Since the pioneering work performed by Boman et al. [12,14] in the area of modelling, the continuous roll-forming process in ALE formalism, relentless breakthroughs have been made. First, Boman et al. investigated a specific strategy for the case of a U-channel: the initially-flat strip is bent between the rolls of the mill like in a

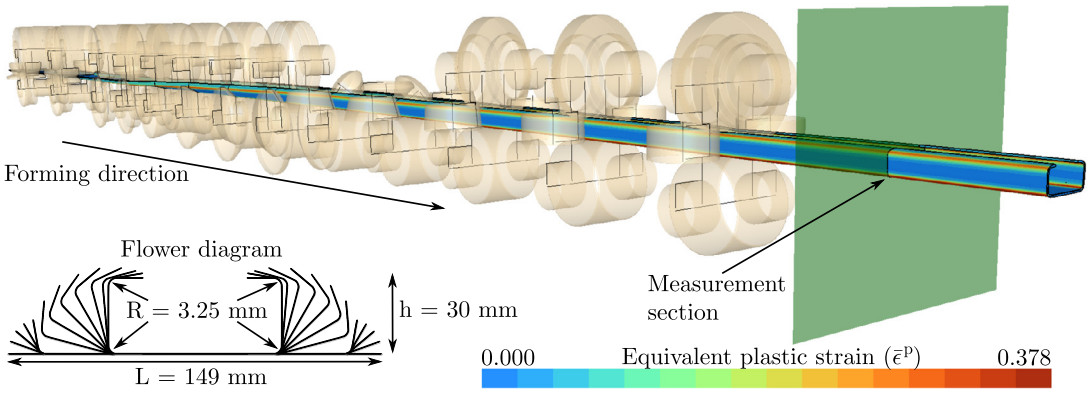

Fig. 2. Illustration of the final stationary state of an ALE roll forming simulation of a C-channel as proposed in [4] with the continuous method using METAFOR (sheet length = 5000 mm).

deep-drawing process, i.e. upper and lower rolls were initially moved apart in transverse directions and the initial flat strip set down between the rolls is then bent as required while moving back the rolls to their real position [12]. However, such a method cannot be readily extended to more complex study cases. In that respect, a more efficient and versatile method has been proposed: the numerical simulation starts with an initial guess on the final sheet geometry inside the mill, leading to the desired steady state [14]. This initial geometry is built by the interpolation from the flower diagram of the mill, simplifying the beginning of the simulation in terms of contact conditions. The flower diagram, which directly comes from the design strategy [3], shows the superposition of the cross-sectional shapes imposed by each forming stand (see, e.g., Fig. 2).

Besides, it is worth noting that, since roll forming features a large characteristic forming time due to the length of the mill, using an explicit time integration scheme cannot be considered as the best option. Such an explicit time integration technology, which is usually used in the finite element codes available on the market for forming applications, cannot provide a fast and cost-effective solution due to its intrinsic limitations — the smallness of the critical time increment — for simulating the roll-forming process. The resulting huge number of small time increments required by an explicit scheme should induce a time-prohibitive and even certainly not affordable endeavour for the case of industrial forming mills, as considered in the present paper. Accordingly, dealing with such demanding industrial applications in a reasonable computational time should be restricted to an implicit time integration scheme.

All these developments have been implemented in METAFOR [5,6], an in-house nonlinear finite element code of the Aerospace & Mechanical Engineering Department of the University of Liège, Belgium. The considered numerical techniques should help FEA to become a systematic integrative part in the design strategy of the roll-forming process.

In our previous works [12,14,15], an experimental validation was performed with both ALE and Lagrangian formalisms for a simple U-channel forming, and some preliminary simulation results were presented for a tubular rocker panel which is roll-formed from a real post-cut industrial mill. In the present paper, the research study is going one step further: an in-depth numerical analysis is detailed for the rocker panel with a particular emphasis on the continuous-type forming using both ALE and Lagrangian simulations. ALE and Lagrangian results are quite close to each other. This article also aims at discussing the numerical problematic aspects in simulating such a forming process. We show that, contrary to the Lagrangian formalism, the ALE formalism is a technique which is, as presented here, tailored to model efficiently the continuous-type roll-forming process. In an industrial context, one of its most attractive features is distinctly its ease of use for simulating the forming process of highly complex mills.

The paper is structured as follows: Sections 2 and 3 introduce the general methodologies implanted in METAFOR for the modelling of the roll-forming process using respectively the Lagrangian and ALE formalisms, while discussing advantages and drawbacks from the two approaches. Section 4 provides a brief overview of the present parallelism implementation in METAFOR. In Section 5, Lagrangian and ALE results are compared for the forming of a tubular rocker panel. Advantages of the roll-forming simulation in ALE formalism are highlighted. Eventually, Section 6 presents the conclusions and prospects that can be drawn from this work.

2. General methodologies for Lagrangian modelling

2.1. Progress of the simulation

In METAFOR, the progress of a Lagrangian roll-forming simulation is typically as follows [7,14,15]: during the initial step, the flat pre-cut strip lies in front of the roll-forming mill (see Fig. 1). It is driven forward by a prescribed displacement on the front and rear sides in order to achieve the first contact with the rolls. Then, artificial boundary conditions are adopted, until friction with the rotating rolls is sufficient to drive the sheet. Similarly, artificial boundary conditions are required when releasing the sheet from the two last forming stands of the mill to eliminate any unwanted rigid body motion.

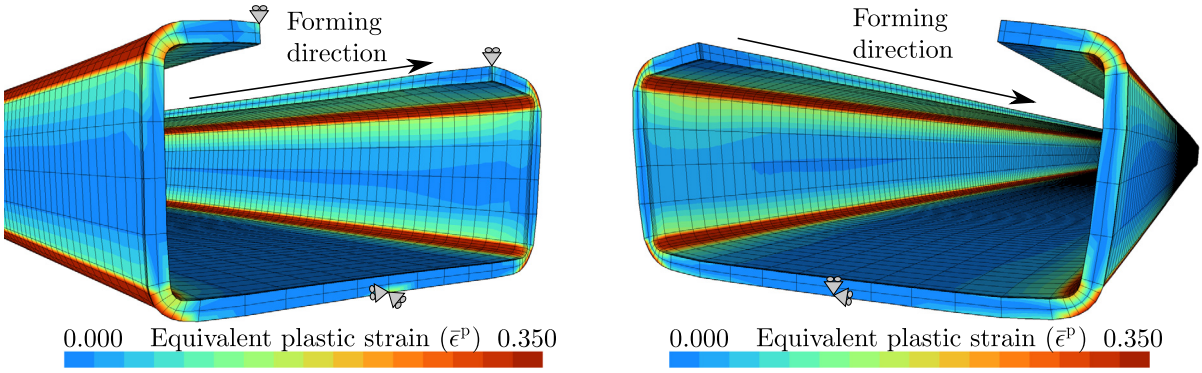

(a) Front section. (b) Rear section.

Fig. 3. Boundary conditions prescribed during the final "springback step", after the strip is released from the mill. Forming of a C-channel.

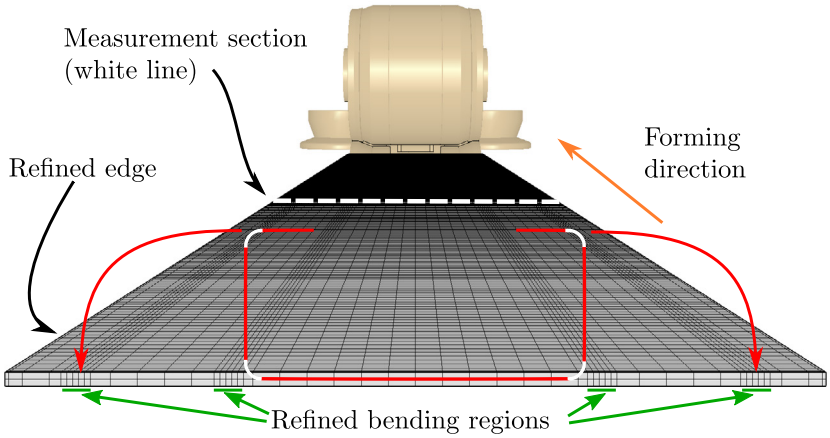

Fig. 4. Building of the initial Lagrangian mesh from the final section of a given flower diagram. Forming of a C-channel.

Otherwise, a commonly used simplification in the literature [9,16–23] is to prescribe the forming velocity during the entire process either by driving the forming tools while some artificial fixations are prescribed on some strip nodes or on the contrary by driving the sheet through the forming stands.

After roll forming, when the strip is completely out of the tooling of the mill, a final step, intended to relax as far as possible the stresses induced by the artificial boundary conditions, is performed. This additional step is said to be a "springback step". It enables us to ensure that the roll-formed product is quasi-totally free from external forces and hence to capture accurately the springback. In that respect, some isostatic boundary conditions are prescribed on the strip as they are depicted in Fig. 3. Besides, damping elements are introduced because of the transient vibrations coming from the boundary conditions switching. Like for the roll forming simulation, a Chung–Hulbert dynamic implicit scheme [25] is adopted in the final step.

2.2. Mesh

As it can be seen in Fig. 4, the initially flat sheet mesh is refined in the bent areas extracted from the final section geometry of the flower diagram, coming from the roll-design software COPRA RF [4]. Besides, the mesh density along the forming direction is constant, except near the front and rear extremities of the strip for numerical purposes. Indeed, it enables us to deal with contact conditions more easily.

The time evolution of strains, stresses and the section geometry is continuously recorded in the middle cross-section of the sheet, named "measurement section" in Fig. 4. The middle location is definitely the best choice to accurately depict the continuous roll-forming process case because it is the least influenced by the front and rear boundary regions of the strip.

A fine mesh all along the forming direction is required to deal rightly with the contact between the strip and the tools. Otherwise, since node-to-surface contact elements are used, a "too coarse" mesh would result, on the one hand, in large penetrations of the strip into the tool surfaces and, in turn, in a poor forming quality. On the other hand, unstable contact conditions involving too few nodes could occur, resulting in unwanted large time increment variations during the time integration. Besides, it is important to note that refining the mesh along the forming direction in the close vicinity of the

"measurement section" is not an option to get more accurate results. In practice, for such a case, our numerical experiments have indicated that large longitudinal variations may be induced in the observed fields. Consequently, a uniform fine mesh along the forming direction is needed to get at once accurate results in the measurement middle section and right contact conditions.

2.3. Difficulties in Lagrangian roll-forming models

Simulating the roll-forming process with the Lagrangian formalism involves several other difficulties. Some of them are listed below.

- The size of the model rapidly increases with the strip length due to the large number of finite elements that is required to get an accurate solution, leading thus to time-consuming simulations. The only remaining and generally adopted solution for performing Lagrangian simulations in a practically reasonable time is to shorten the strip length, hoping it really depicts the continuous forming process since the front and tail ends are not held simultaneously between pairs of neighbouring rolls. Nonetheless, it is well-recognized that the pre-cut forming method usually exhibits larger end-flares.
- Some transient dynamic vibrations may occur each time the sheet hits a forming tool and enters a forming stand. In addition, during the beginning of the simulation, the contact of the initially flat strip with the rolls may lead to some vibrations because of its low structural stiffness. The useless computation of these vibrations is responsible for a severe slow down of the convergence rate of the time integration process and hence a waste of CPU time.
- The Lagrangian approach is sometimes absolutely ineffective if the mill is originally designed for the continuous forming method. Indeed, when the front of the pre-cut strip hits the tooling, it is sometimes unable to enter rightly the forming stand without any help from the operator or some additional guides between the stands. If the latter are not included in the numerical model, these impacts produce complex contact conditions that lead to an early end of the simulation.
- The short sheet is certainly subject to overharden if some artificial boundary conditions are prescribed during forming.
- All the nodes on the surface of the strip are potentially in contact with, at least, as many tools as forming stands, resulting in a costly contact detection.

3. General methodologies for ALE modelling

3.1. General ALE algorithm

The ALE description enables the computational mesh to be moved in some specific manner, regardless of the material motion. Both classical Lagrangian and Eulerian formalisms are particular cases of the ALE formulation prescribing the mesh velocity either equal to the material one or to zero [26].

In the ALE formalism, a new grid coordinate system $R_{\boldsymbol{\chi}}$ is defined and the conservation laws and the constitutive equations are rewritten in terms of the new coordinates $\boldsymbol{\chi}$:
Mass:

$$\left.\frac{\partial \rho}{\partial t}\right|_{\boldsymbol{\chi}} + \boldsymbol{c}\cdot\nabla\rho + \rho\,\nabla\cdot\boldsymbol{v} = 0 \tag{1}$$

Momentum:

$$\rho\left(\left.\frac{\partial \boldsymbol{v}}{\partial t}\right|_{\boldsymbol{\chi}} + (\boldsymbol{c}\cdot\nabla)\,\boldsymbol{v}\right) = \nabla\cdot\boldsymbol{\sigma} + \rho\,\boldsymbol{b} \tag{2}$$

Energy:

$$\rho\left(\left.\frac{\partial u}{\partial t}\right|_{\boldsymbol{\chi}} + \boldsymbol{c}\cdot\nabla u\right) = \boldsymbol{\sigma} : \mathbf{D} + \rho\, r + \nabla\cdot\boldsymbol{q} \tag{3}$$

Material:

$$\left.\frac{\partial \boldsymbol{\sigma}}{\partial t}\right|_{\boldsymbol{\chi}} + (\boldsymbol{c}\cdot\nabla)\,\boldsymbol{\sigma} = \mathcal{H} : \mathbf{D} + \mathbf{W}\boldsymbol{\sigma} - \boldsymbol{\sigma}\,\mathbf{W} \tag{4}$$

where ρ is the mass density, $\boldsymbol{\sigma}$ is the Cauchy stress tensor, $\boldsymbol{b}$ and r are the specific body forces and heat sources, u is the specific internal energy, $\mathbf{D}$ and $\mathbf{W}$ are the symmetric and antisymmetric parts of the velocity gradient tensor, $\boldsymbol{q}$ is the heat flux, and $\mathcal{H}$ is a material tensor depending on the constitutive parameters, the stresses and the loading history. The last two terms in Equation (4) result from the particular choice of the Jaumann's objective time derivative.

The convective velocity $\boldsymbol{c} = \boldsymbol{v} - \boldsymbol{v}^*$ is the difference between the material velocity $\boldsymbol{v}$ and the mesh velocity $\boldsymbol{v}^*$. In the case of nonlinear problems, such as metal-forming simulations, $\boldsymbol{v}^*$ should ideally depend on the solution. It is thus an additional unknown of the latter system of equations.

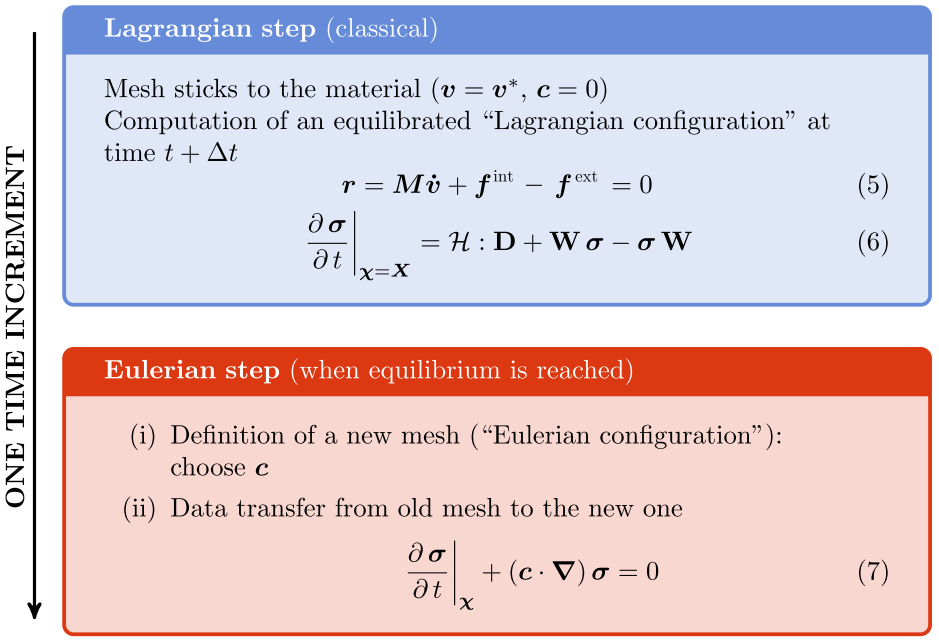

Fig. 5. Operator-split flowchart for the ALE resolution scheme.

In METAFOR, the ALE resolution scheme relies on an operator-split methodology (see Fig. 5) [26,27]. In other words, each time increment, from time t to $t + \Delta t$, is divided into two successive steps: a purely Lagrangian one followed, once the equilibrium is reached, by an Eulerian one. During the Lagrangian step, the mesh follows the material motion and the classical Lagrangian formalism is used ($\boldsymbol{v} = \boldsymbol{v}^*$, $\boldsymbol{c} = 0$). Equation (5) is the discretized form of the principle of virtual work where $\boldsymbol{r}$, $\boldsymbol{f}^{\text{int}}$ and $\boldsymbol{f}^{\text{ext}}$ stand for the vectors of residual forces, internal forces and external forces, respectively, and $\boldsymbol{M}$ is the mass matrix. The detailed expressions of the latter quantities are classical (see, e.g., [6]). In this Lagrangian step, the constitutive equation is given by Equation (6) where $\boldsymbol{X}$ denotes the material coordinates. During the Eulerian step, a new mesh is created by relocating the nodes of the Lagrangian solution. Numerical results, such as stresses and internal state variables of the material, are then transferred from the old Lagrangian mesh to the new Eulerian one. This transfer step is expressed by Equation (7). Eventually, friction forces are computed on the new mesh and the mass matrix is re-evaluated before starting the next time increment.

Furthermore, if the same mesh, the same boundary conditions and the same parameters are considered, an ALE simulation obviously outweighs the cost of a purely Lagrangian one in terms of memory and CPU time since the effort involved in computing the additional Eulerian step is not insignificant with respect to the Lagrangian one. Consequently, an ALE model must always be optimized to take advantage of the specific kinematics of the mesh.

3.2. Mesh management

The generation of the initial ALE mesh of the sheet, which already lies between the rolls of the forming mill, is a decisive step for an efficient ALE model. An example is represented in Fig. 6. The idea is to build a first guess of the final geometry inside the mill from a given flower diagram. The latter is thus a new input of the FE model that directly comes from the design strategy of the process. It is important to understand that this initial geometry is only a starting point of the simulation that could be chosen among many others and the resulting final stationary solution does not depend on it. In addition, one can expect from this strategy to be a cost-efficient attempt since the initial mesh is very close to its final configuration.

The initial mesh is automatically built as follows: first, each cross-section of the flower diagram is drawn at the longitudinal coordinate of the corresponding stand. The first and the final ones are duplicated in order to model inlet and outlet zones. These artefacts play a crucial role in the simulation. The inlet is important to move the boundary conditions away from the first stand. The outlet enables us to extract the final cross-sectional shape of the roll-formed product. In fact, contrary to the Lagrangian model, there is no additional "springback step" during the time integration. The outlet length is chosen with the aim to minimize the influence of both the last set of tools and the boundary conditions (the material flow prescribed at the downstream Eulerian boundary) on the springback. Usually, from our experience, measuring the cross-sectional shape at one downstream inter-stand distance from the last stand is a good choice (see Fig. 2). Once the sections are in place, they are uni-dimensionally meshed considering all the bending radii that require a larger node density. Next, these meshed curves are "thickened", projecting their nodes on both sides using half the sheet thickness (t) value.

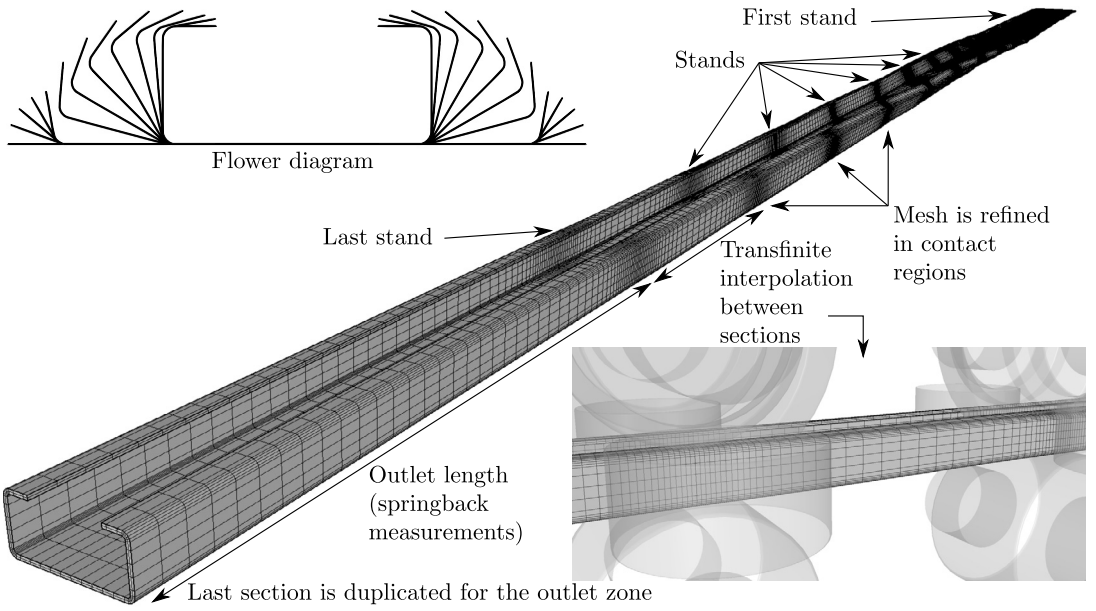

Fig. 6. Building of the 3D initial ALE mesh from a given flower diagram. Forming of a C-channel.

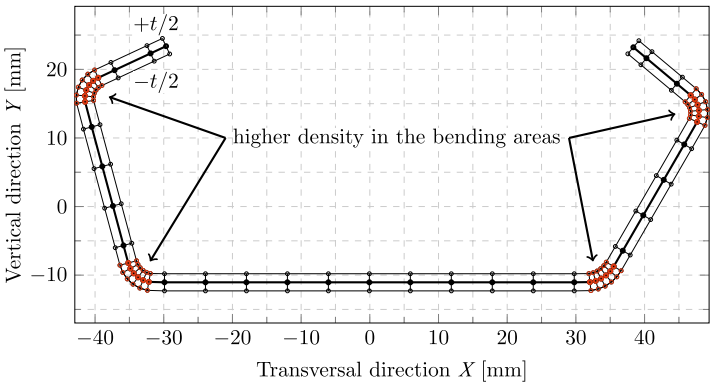

Fig. 7. Building of the 2D initial ALE mesh from a given section of the flower diagram. Forming of a C-channel (section #12).

A 2D mesh is then obtained by transfinite mapping prescribing the desired number of elements through the thickness (see Fig. 7). Eventually, a 3D mesh is interpolated between the different stands using cubic spline curves, the tangents of which are chosen to be aligned with the forming direction (see Fig. 6).

During the roll-forming simulation, the ALE mesh is almost fixed — and is said to be quasi-Eulerian — along the forming direction but is free to move in transverse directions (see Fig. 8). The ALE domain is delimited by Eulerian boundaries at the front and the rear of the roll forming machine where the material flow is prescribed. A detailed description on the mesh management of the Eulerian step may be found in [14,28].

3.3. Convective step

The data transfer between the Lagrangian and Eulerian meshes requires a fast but accurate data transfer algorithm and must be applied to the values defined at the Gauss points (e.g., stresses or the equivalent plastic strain) and to the values defined at the nodes of the mesh (velocities, accelerations, etc.) [27,29–31]. This problem is similar to the one encountered in a complete remeshing procedure except that in this case both meshes have the same topology, which means that they have the same number of nodes and each node has the same number of neighbouring elements. This latter property is extensively used in the ALE algorithm to make the transfer much faster than in a complete remeshing context.

If σ denotes one scalar Gauss point value, such as one component of the Cauchy stress tensor $\boldsymbol{\sigma}$, the algorithm consists in writing the following equality over the total deformed volume $\mathbb{V}$ of the mesh:

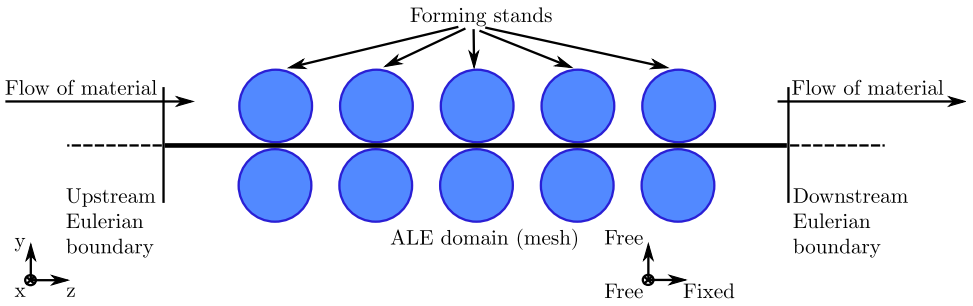

Fig. 8. Schematic mesh management in the ALE roll forming model.

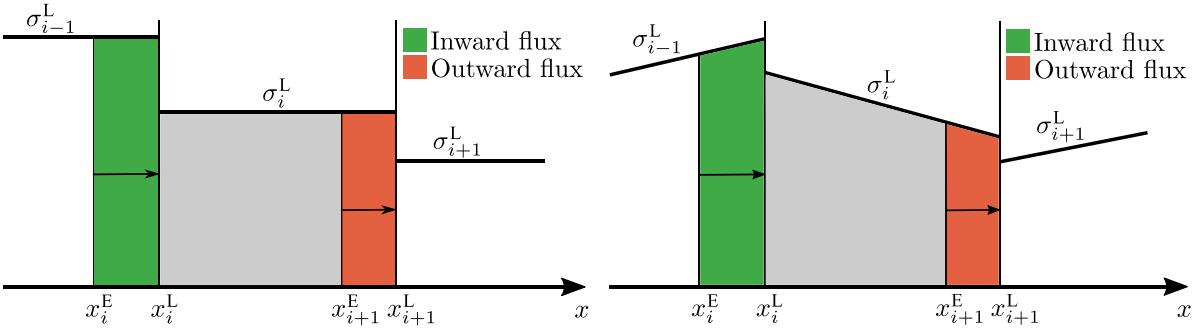

(a) Constant reconstruction per element.

(b) Linear reconstruction per element.

Fig. 9. Reconstruction of σ^{L} in the 1D case.

$$\int_{\mathbb{V}} \sigma^{E}\,d\mathbb{V} = \int_{\mathbb{V}} \sigma^{L}\,d\mathbb{V} \tag{8}$$

where the superscripts L and E designate the values defined on the Lagrangian and the Eulerian meshes, respectively.

In the case of 8-node bricks with eight Gauss points, each finite element of the mesh is divided into eight subcells surrounding each quadrature point. An auxiliary mesh composed of all these subcells around the Gauss points is built during the preprocessing phase of the computation. Then, for each transfer, a continuous field per element $\sigma^{L}(\boldsymbol{x})$ is reconstructed from the pointwise-defined values of σ^{L}:

$$\sigma^{L}(\boldsymbol{x}) = \bar{\sigma}^{L} + \nabla\sigma^{L} \cdot (\boldsymbol{x} - \bar{\boldsymbol{x}}) \tag{9}$$

where $\nabla\sigma^{L}$ is the unknown gradient of σ^{L}, which is supposed to be constant over each cell. The values $\bar{\boldsymbol{x}}$ and $\bar{\sigma}^{L}$ are the position of the gravity centre of the cell and the value of σ^{L} at that point, respectively. If $\sigma^{L}(\boldsymbol{x})$ is chosen constant over each cell ($\nabla\sigma^{L} = 0$), the resulting transfer scheme will be first-order accurate (see Fig. 9a). If the reconstruction is linear per element, which requires the costly computation of an approximation of the gradient of $\sigma^{L}(\boldsymbol{x})$, the scheme will be second-order accurate (see Fig. 9b).

By considering that $\sigma^{E}(\boldsymbol{x})$ is constant over each element, Equation (8) may be used to express the new value of σ in cell i (namely σ^{E}_{i}) as a function of the previous values of σ in the cell (denoted σ^{L}_{i}) and in its N_i neighbours:

$$\sigma^{E}_{i} = \frac{1}{V^{E}_{i}} \left(\sigma^{L}_{i} V^{L}_{i} - \sum_{j=1}^{N_i} \Delta\sigma_{ji} \right) \tag{10}$$

where $V^{E,L}_{i}$ is the volume of the cell in the Eulerian (E) or Lagrangian (L) configuration. The term $\Delta\sigma_{ji}$ is the outward flux of σ through the boundary j of element i.

Similarly to Gauss point values, the nodal values must be also transferred from the Lagrangian mesh to the Eulerian mesh. For the sake of simplicity, it seems obvious to use the same algorithm as for the values at Gauss points. In the case of 8 quadrature points, a nodal auxiliary mesh may be easily constructed by merging the previous neighbouring transfer cells located around the nodes of the primary finite element mesh.

In our work, a second-order convection scheme described in [31] is adopted and the deformation gradient tensor $\mathbf{F}$ is convected to be able to compute the longitudinal strains despite the fact that the mesh does not follow the material's motion.

3.4. Key features for-roll forming simulation

Advantages of the ALE formalism for the roll-forming simulation are multiple:

- By its specific construction, it is representative of a continuous roll-forming process for the entire mill since the contributions of all the forming tools are taken into account simultaneously.
- Unlike the Lagrangian case, the length of the finite elements can vary along the forming direction. Since the mesh is quasi-Eulerian, only bending regions and contact areas, clearly delimited for such a forming process, require a fine mesh to improve the quality of the results. Element size in the inter-stand regions can be, without any loss of accuracy, chosen much larger since smaller deformation gradients are expected there (see Fig. 6). As a result, the total size of the model can be kept relatively reasonable considering that the entire length of the forming mill is modelled.
- Thanks to the quasi-Eulerian motion of the mesh, a very limited number of nodes is concerned with the contact algorithm and each node may be in contact with its own single forming stand.
- Compared to a Lagrangian model, the complex contact conditions resulting from the sheet entry into the successive rolling tools are completely overcome.
- The complex boundary conditions that have to be defined to drive the Lagrangian sheet before, after and sometimes in the process of roll forming are useless in an ALE model.
- Since a given constant forming velocity is prescribed at the front and the rear sections of the ALE mesh during all the simulation, frictionless contact conditions can be assumed.

In contrast to the Lagrangian model, it is worth noting that the evolution of the observed fields along the forming direction is obtained from the spatial evolution of the final configuration at the end of the simulation.

4. Parallelism implementation

With the aim to meet the computational resource needs of the simulations, Shared-Memory Parallelism (SMP) has been introduced into the code METAFOR. Intel Threading Building Blocks (Intel TBB) [32], a C++ template library for shared memory programming, has been adopted. In contrast with OpenMP standard [33], it is a library dedicated to highly object-oriented code, thereby minimizing the complexity introduced by adding parallelism to METAFOR.

In the present state of the code, excepted for the contact detection and the Eulerian step, the most CPU-intensive algorithms (external, internal and inertial forces computation, tangent stiffness matrix computation and linear system solver) are parallel. The linear solver is the Pardiso Solver packaged with the Intel Compiler (also called DSS) [34,35].

In conclusion, the parallelism implanted so far into METAFOR represents a first step. Further development and research are needed to harness the capabilities of parallel computing and thereby shorten even more the computation time.

5. Numerical example

The present example emphasizes the advantages of the ALE model, especially its ease of use, to simulate a long and complex forming mill. A non-symmetric tubular rocker panel (initial dimensions: width = 167 mm, thickness = 1.5 mm) is formed by 16 stands with an inter-stand distance set to 350 mm, giving a total length of 5600 mm. The mill, which is a real industrial continuous roll forming line, is represented in Fig. 10 with its flower diagram. We have previously shown in [14] the feasibility of this example using the ALE formalism, but numerical results were not explored in detail.

5.1. Parameters of the numerical models

In the frame of this work, the considered material is a high-strength DP980 steel, with Young's modulus $E = 210$ GPa and Poisson's ratio $\nu = 0.3$, characterised with the following Swift hardening law:

$$\sigma_y = 1626\,(0.00487 + \bar{\epsilon}^{\mathrm{p}})^{0.17} \tag{11}$$

where the initial yield stress $\sigma_{0.2} = 697.34$ MPa. The constitutive material behaviour has been studied extensively by Flores and Habraken [36,37] in the scope of the U-channel forming described in [14]. In our study, a simplified isotropic law is adopted. According to Bui et al. [7], kinematic hardening may be safely neglected since no plastic unbending occurs during the forming process.

In respect of the ALE model, the sheet is 6150 mm long. The outlet length of the strip is set to one inter-stand distance plus 200 mm. The springback is measured on the cross-section located at one downstream inter-stand distance from the last forming stand of the mill, i.e. 200 mm upstream from the mesh boundary. The size of the finite elements varies from 3 to 15 mm along the forming direction. Along the transverse direction, the background mesh size is 6 mm, except in the bending zones that are meshed finely with 5 elements. At the interfaces between the strip and the rolls, friction is taken into account with a Coulomb coefficient $\mu = 0.2$.

Regarding the Lagrangian model, a frictionless contact is assumed for simplicity and the forming tools are moved along the sheet (length = 1060 mm $\approx 3\times$ inter-stand distance). A zero displacement is prescribed at the front and back ends of the sheet in the forming direction. The Lagrangian strip is uniformly meshed along the forming direction with 3-mm-long

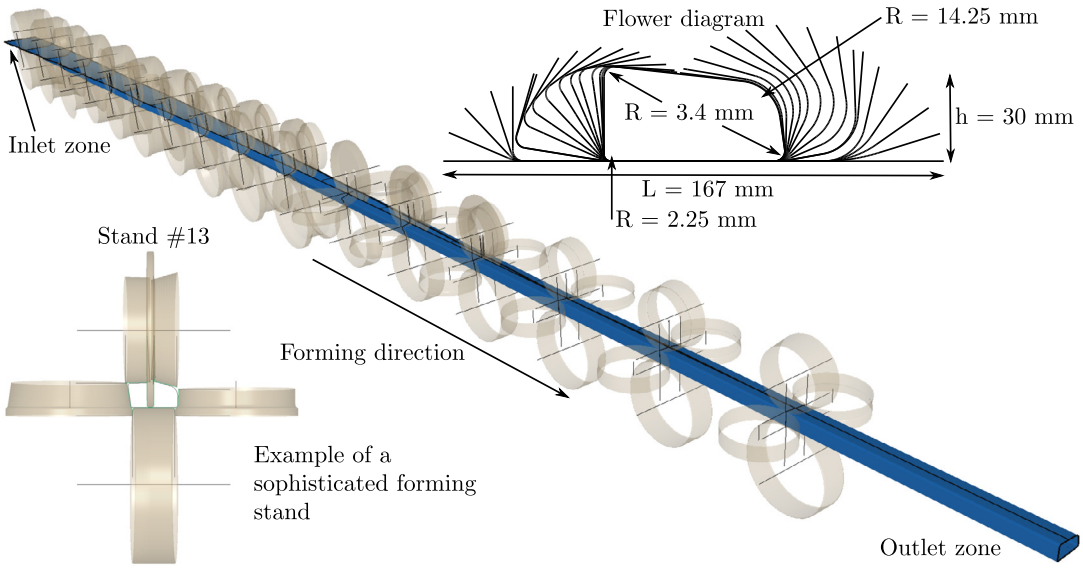

Fig. 10. Initial ALE geometry and flower diagram of a tubular rocker panel as proposed in [4] (sheet length = 6150 mm = 1.10 L_{mill}).

Table 1
Parameters of Lagrangian and ALE meshes. Forming of a rocker panel.

		Lagrangian	ALE
Number of elements through the thickness		2	2
Size of the mesh far from the rolls along the forming direction	[mm]	3	15
Size of the mesh near the rolls along the forming direction	[mm]	(3)	3
Mesh along the transverse direction:			
Background mesh size	[mm]	6	6
Number of elements in the bending areas		5	5
Sheet length		0.19 L_{mill}	1.10 L_{mill}

elements. Along the transverse direction, the background mesh size is 6 mm, except in the bending areas that are discretized finely with 5 elements.

Both Lagrangian and ALE meshes are made up of 2 layers of Enhanced Assumed Strain (EAS) elements [38] through the thickness. For the purpose of the present study, it is important to note that no numerical sensitivity analysis has been carried out. The emphasis is placed on providing results with hopefully enough quality and confidence in an acceptable computational time so as to compare between each other. In that respect, similar mesh density parameters are adopted for both models, except for the inter-stand regions of the ALE mesh where longer elements are obviously considered.

The considered numerical parameters of both Lagrangian and ALE meshes are summed up in Table 1. The Lagrangian model contains 35,280 finite elements and the ALE one 73,226.

The rolling tools are considered rigid and the penalty method is used to model the contact between the rolls and the strip.

Concerning the time integration, a Chung–Hulbert dynamic implicit scheme [25] is adopted in both ALE and Lagrangian cases (forming velocity = 200 mm/s).

The numerical simulations are performed on one compute node which consists of two 6-core Intel Xeon Westmere X5650 2.66 GHz processors, giving 12 cores in total per node with a memory of 48 Gbytes.

5.2. Results and discussion

The ALE stationary solution is obtained after a total convective displacement of 1.2 times the sheet length in 4310 time increments, 11,539 mechanical iterations and 11 d 5 h of CPU time. The Lagrangian simulation is computed in 9322 time increments, 28,519 mechanical iterations and 1 d 3 h 40 m of CPU time. Although the Lagrangian simulation clearly outperforms the ALE one in terms of computational times, this cannot be pursued in this very case in a right-first-time operation (a costly step-by-step approach is needed, as it will be explained later in Section 5.3).

Fig. 11 presents snapshots of the downstream strip from the ALE simulation. The initial state, which geometrically corresponds to the desired shape, is depicted in Fig. 11a. During a long transient phase, the material flows through the quasi-Eulerian mesh from upstream to downstream, inducing some transient oscillations of the mesh and the fields as they can be seen in Fig. 11b. Finally, once the effect of all the stands reaches the downstream extremity of the sheet, stabilization

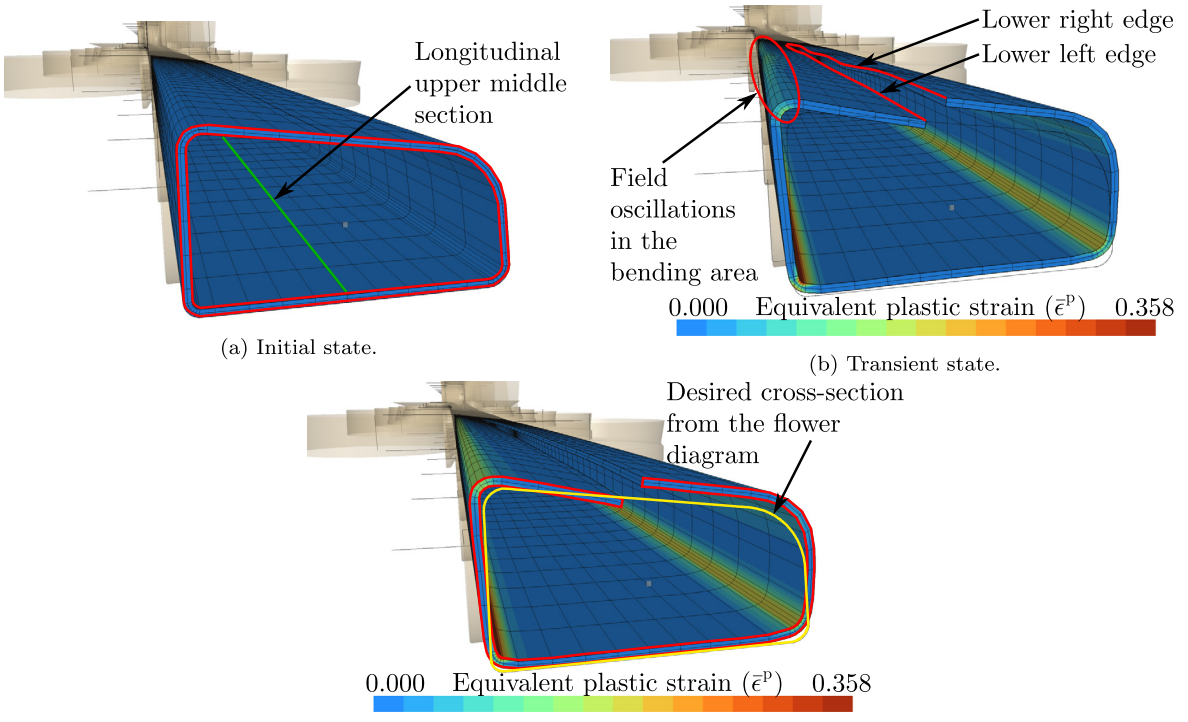

(a) Initial state.

(b) Transient state.

(c) Final stationary state.

Fig. 11. Initial, transient and final stationary states observed from a downstream point of view. Forming of a rocker panel (ALE model).

occurs and a stationary solution is achieved (see Fig. 11c). As one can see in Figs. 11b and 11c, the ALE model as well as the Lagrangian one do not include the welding of the closed section yet, enabling us to measure the springback.

Edge and middle section longitudinal strains (ε_{ZZ}^{GL}) along the forming direction are measured on the upper side of the sheet and are plotted in Fig. 12. Except before the first stand, the red ALE and blue Lagrangian curves are very similar and the maxima values are close to each other. Then, the steep slope of the strain peaks, each one located very close to each forming stand, has to be pointed out and demonstrates the notable sensitivity of both ALE and Lagrangian models. Finally, the major discrepancies are located in the inlet region and are as a consequence irrelevant. Actually, the results within this inlet region are simply disturbed by the different considered boundary conditions.

Figs. 13 and 14 show the Lagrangian path followed by the strip along the forming direction and the corresponding ALE final shape on, respectively, the middle section and the left edge of the sheet. Although the curves are, once more, globally similar, ensuring confidence in the two models, several discrepancies are observable. First, an increasing gap between the final ALE shape and the Lagrangian path may be noticed on the edge of the sheet in the downstream part of the mill (from stand #13 to the end of the mill). Secondly, the Lagrangian curves exhibit some additional high-frequency oscillations at the inlet zone. Furthermore, they are sometimes more uneven with respect to the ALE curves, because of the multiple “shocks” when the front of the sheet hits the rolls.

As regards the final cross-sectional shape including springback, the numerical models yield slight differences between each other. From Fig. 15, one can observe that the ALE and Lagrangian cross-sections do match each other, except for the left flange. The Lagrangian model gives a more open shape than the ALE one. Comparing with the desired shape, both left and right flanges exhibit a notable springback since the welding of the closed section is not modelled. Moreover, the computed bending radii near the web are similar but much larger than the desired ones.

In Fig. 16, the cross-section extracted at the longitudinal coordinate of the stand #13 from the ALE and Lagrangian simulations is compared to the corresponding desired section of the flower diagram. The computed radii of the bending areas do not perfectly fit the desired ones despite the fact that the lateral surfaces of the strip edges are held by the upper middle roll (see Fig. 10). Moreover, the bending angle of the left ALE flange is smaller than the Lagrangian one, confirming the previous observation on the left shape edge along the forming direction. It is worth mentioning that there is no lower tooling to held the upper side of the flange in the last forming stands.

5.3. Discussion of advantages and disadvantages of both ALE and Lagrangian models

From the computational times and the results discussion presented above, a well-founded question arises: why cannot one be satisfied with the Lagrangian model for the simulation of the continuous-type roll-forming process? Even if the ALE simulation is the most CPU-expensive one, it is nevertheless a more appropriate model. Several reasons can be formulated.

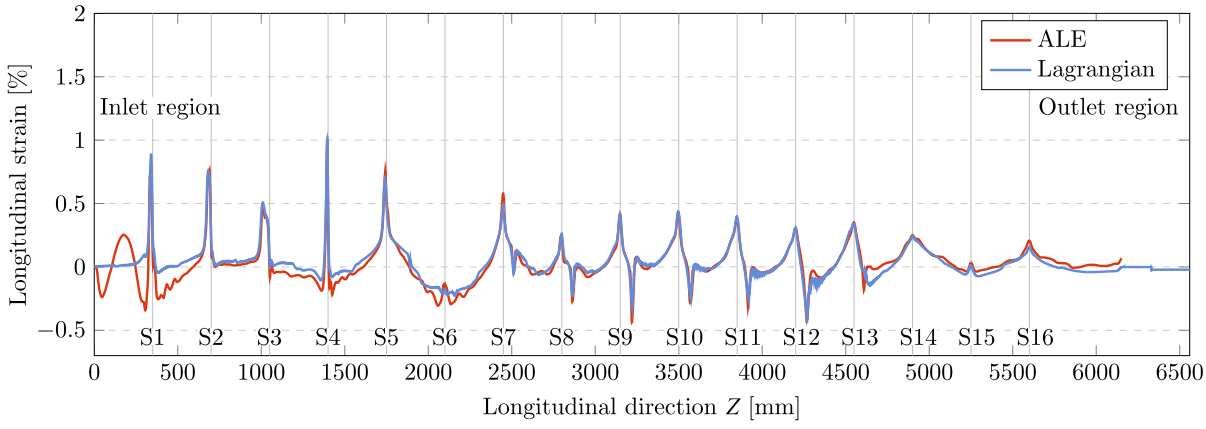

(a) Left edge.

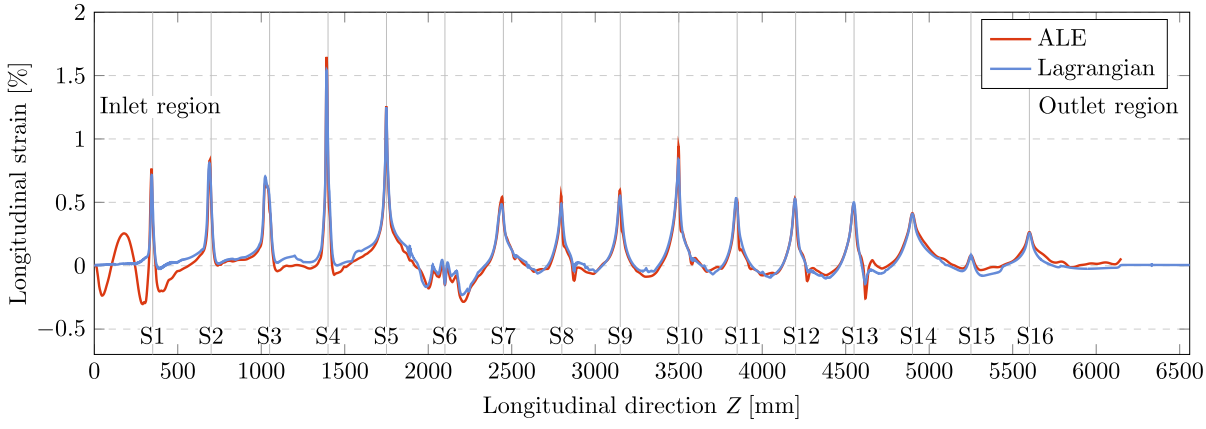

(b) Right edge.

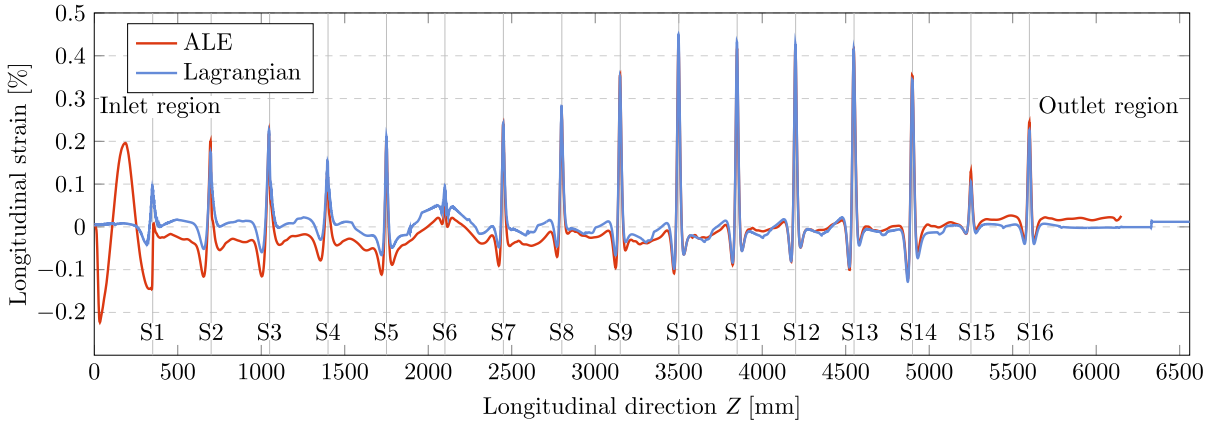

(c) Middle section.

Fig. 12. Longitudinal strain ε_{ZZ}^{GL} in the longitudinal direction. Forming of a rocker panel.

First, fatal issues were encountered when the Lagrangian sheet is unable to enter between some forming rolls. Such problems are symptomatic of the pre-cut forming method as modelled with a Lagrangian formalism, whereas the mill is originally designed for the continuous-type forming. As it can be seen for instance at stand #7 in Fig. 17a, in this very case, the left flange tip severely hits the upper left roll, bending the sheet in a non-expected way. Even if some boundary conditions can be adapted on the front section in order to modify the way the sheet enters into the next forming stand, there have been many unsuccessful attempts to force the sheet to enter between the rolls. The adopted solution to these Lagrangian specific issues is illustrated in Figs. 17b and 17c. Firstly, the involved stands (stands #7 to #10) are cut

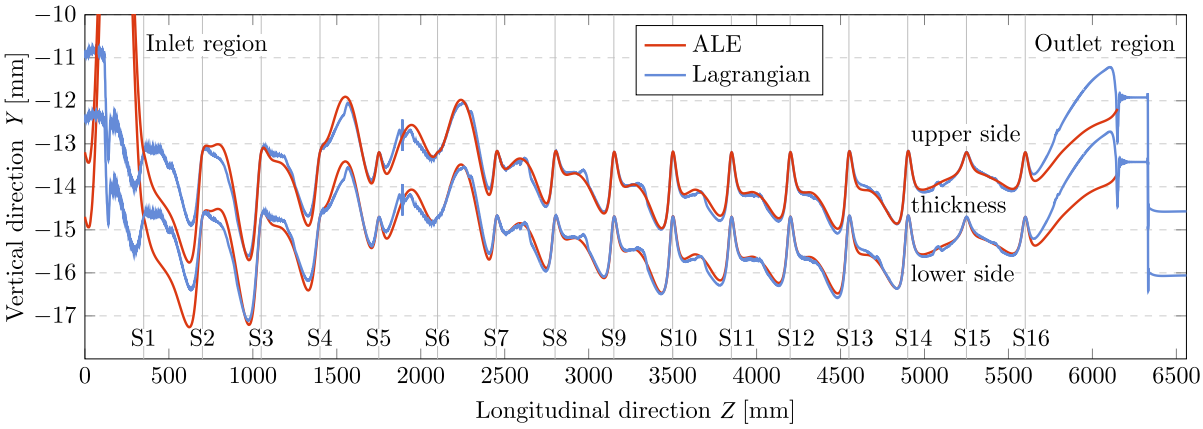

Fig. 13. Shape of the strip (middle section) along the longitudinal direction. Forming of a rocker panel.

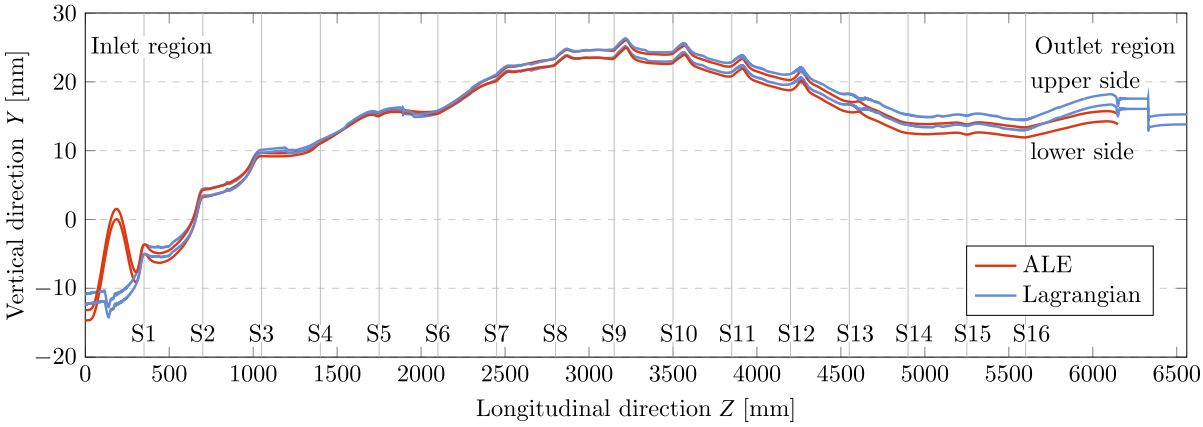

Fig. 14. Shape of the strip (left edge) along the longitudinal direction. Forming of a rocker panel.

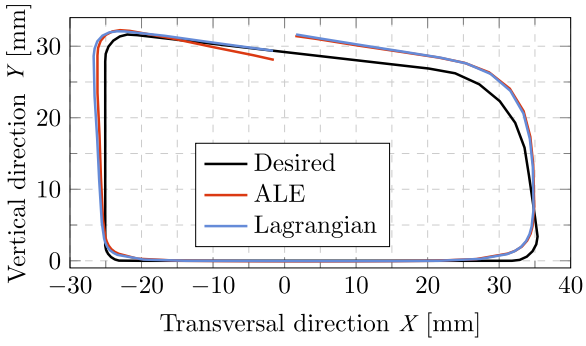

Fig. 15. Final cross-section of a rocker panel including springback.

open, allowing the sheet to enter more easily into the forming stand. Then, the latter is gradually closed to its original configuration, bending the sheet as required. As a result, multiple trials-and-errors had to be conducted to successfully simulate the forming process, leading to a large waste of human time and CPU time. Regarding the ALE model, it is no longer an issue since the mesh of the sheet is already in a right position from the beginning of the simulation.

Secondly, in the frame of Lagrangian modelling, our choices about the boundary conditions management and the sheet length are far from evident, represent a tedious work and may be moreover contestable. These choices influence the slipping of the strip through the rolling tools and thereby the actual forming velocity, not without presenting problems for the time when some boundary conditions have to be set up to bring out the sheet from the mill. For this reason, the model is simplified in assuming frictionless contact and adding some artificial fixations on the strip. Then, since the Lagrangian results may exhibit sensitivity to the pre-cut sheet length, it is not obvious to guess the minimal length that should correspond to

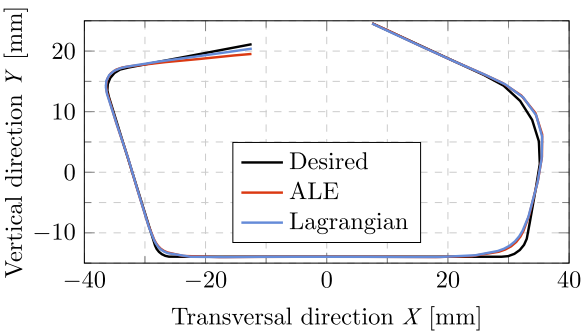

Fig. 16. Cross-section extracted from the stand #13. Forming of a rocker panel.

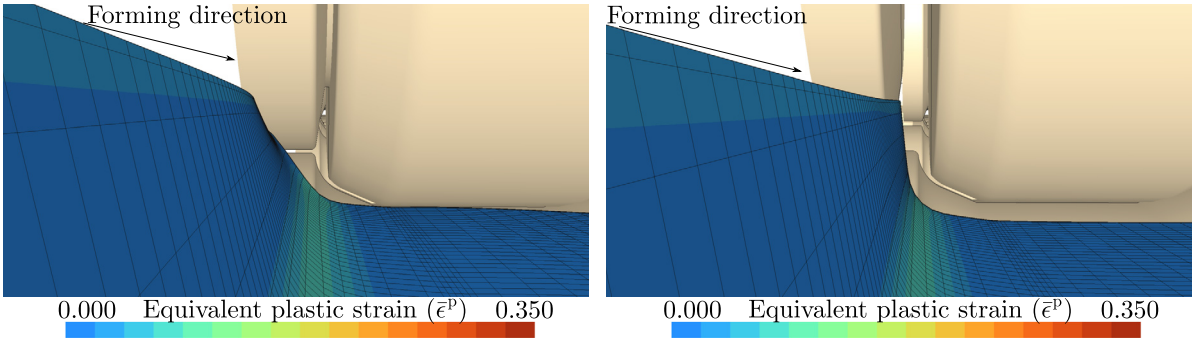

(a) Issue: the left flange tip severely hits the upper roll, bending the sheet in a non-expected way.

(b) Solution part 1: the upper roll is first moved away along its rotating axis.

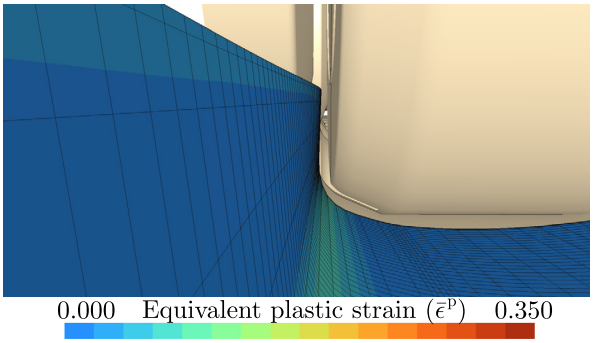

(c) Solution part 2: the upper roll is secondly moved back along its rotating axis, bending the sheet as expected.

Fig. 17. Complex contact conditions at stand #7. Forming of a rocker panel (Lagrangian model).

a continuous roll-forming process. In this very case, as mentioned earlier, it could explain the differences we get between the Lagrangian and ALE results on the final cross-sectional shape and the shape of the left edge along the forming direction. One of the salient points of the ALE model is precisely to consider the simultaneous effect from all the forming tools of the entire mill while pushing away the boundary conditions to the inlet and outlet zones.

Thirdly, the CPU cost in favour of the Lagrangian simulation is not quite surprising given the short modelled sheet length ($0.19\,L_{\mathrm{mill}}$ for the Lagrangian mesh versus $1.10\,L_{\mathrm{mill}}$ for the ALE one). Besides, the size of the ALE mesh could certainly be reduced with longer elements in the inter-stand regions since no mesh optimization has been yet performed.

Finally, it is important to note that the Eulerian step holds for a tremendous contribution (77%) in the global wall-clock time of the ALE simulation. Since this Eulerian step is still computed sequentially in METAFOR, it limits as of today severely the total parallel efficiency. Nonetheless, it reveals a huge potential reduction of CPU time if parallelism was introduced in the Eulerian step routines.

In conclusion, on the one hand, the present industrial application clearly highlights the weaknesses of the Lagrangian-based roll forming model, the latter leading to expensive trial-and-error processes. On the other hand, the ALE-based model

has proven to be more efficient, offering unprecedented ease at simulating the continuous roll-forming process for the entire mill.

6. Conclusions and prospects

High-fidelity finite element simulation is required for providing a deeper understanding of the roll-forming process and predicting shape defects of the final product. In this paper, an effective method based on the ALE formalism has been proposed to numerically simulate the continuous-type forming process for the total length of the mill.

ALE and classical Lagrangian simulations have been successfully carried out for a complex industrial roll forming line. Although the considered ALE model cannot achieve to date any CPU time savings over the Lagrangian one, this delivers essential advantages and represents a valuable tool for the simulation of the continuous-type process. The forming of the tubular rocker panel illustrates the practical necessity of the ALE formalism in numerical roll forming models. Indeed, in contrast to the ALE model, the corresponding Lagrangian model is repeatedly prone to fatal issues when the pre-cut sheet is unable to enter the next forming stand. From the case studied in the present work, it can be stated that the presented ALE and Lagrangian results are generally quite similar despite the fact that the Lagrangian model is not effectively intended to compute the stationary state of the continuous-type process.

From an industrial point of view, the implemented developments address the concerns of roll forming designers. The proposed ALE model is a tool purpose-built for computing the hopefully stationary final state of the continuous forming process for the entire mill, while redefining productivity with effortless set-up tasks compared to the classical Lagrangian approach. Then, parallel computing enables to shorten simulation time responses, giving at the same time a decisive productivity advantage.

Finally, this research work paves the way for some further algorithmic improvements as regards the ALE roll-forming model. A cutting-to-length operation could be added after roll forming, enabling a relevant and more detailed comparison between continuously and pre-cut roll-formed products (e.g., end-flare, longitudinal bow, twist, etc.). In addition, an in-line welding operation could be modelled to close the final section of the tubular rocker panel. Besides, the parallelization of the expensive convection scheme would be worthy of interest and would promise significant reductions in computational times, resulting in a must-have numerical tool.

Acknowledgement

This research work was carried out under grant number 1217573 (STEELPRO) from the Walloon Region, which is gratefully acknowledged.

References

[1] I. Kacar, F. Ozturk, Roll forming applications for automotive industry, in: OTEKON, the 7th Automotive Technologies Congress, Bursa, Turkey, 2014, pp. 26–27.
[2] W. Cubberly, R. Bakerjian, Tool and Manufacturing Engineers Handbook, desk edition, Society of Manufacturing Engineers, 1989.
[3] G. Halmos, Roll Forming Handbook, Manufacturing Engineering and Materials Processing, Taylor & Francis, 2010.
[4] data Sheet Metal Solutions GmbH, COPRA RF, http://www.datam.de/en/products-solutions/roll-forming/.
[5] METAFOR Website, http://metafor.ltas.ulg.ac.be/.
[6] J.-P. Ponthot, Traitement unifié de la mécanique des milieux continus solides en grandes transformations par la méthode des éléments finis (in French), Ph.D. thesis, Université de Liège, Liège, Belgium, 1995.
[7] Q.V. Bui, R. Boman, L. Papeleux, P. Wouters, R. Kergen, G. Daolio, P. Duroux, P. Flores, A.-M. Habraken, J.-P. Ponthot, Springback and twist prediction of roll formed parts, in: Proceedings of IDDRG 2006: International Deep Drawing Research Group Conference, Porto, Portugal, 2006, pp. 567–574.
[8] M. Sheikh, R. Palavilayil, An assessment of finite element software for application to the roll-forming process, J. Mater. Process. Technol. 180 (1) (2006) 221–232.
[9] T. Dutton, P. Richardson, G. Duffett, Simulating the complete forming sequence for a roll formed automotive component using ls-dyna, in: RollFORM'09: 1st International Congress on Roll Forming, Bilbao, Spain, 2009, pp. 49–55.
[10] B. Joo, H. Lee, D. Kim, Y. Moon, A study on forming characteristics of roll forming process with high strength steel, in: The 8th International Conference and Workshop on Numerical Simulation of 3D Sheet Metal Forming Processes, NUMISHEET 2011, vol. 1383, AIP Publishing, 2011, pp. 1034–1040.
[11] J. Falsafi, E. Demirci, V. Silberschmidt, Numerical study of strain-rate effect in cold rolls forming of steel, J. Phys. Conf. Ser. 451 (2013) 12041–12047, IOP Publishing.
[12] R. Boman, L. Papeleux, Q.V. Bui, J.-P. Ponthot, Application of the arbitrary Lagrangian Eulerian formulation to the numerical simulation of cold roll forming process, in: Proceedings of the 11th International Conference on Metal Forming 2006, J. Mater. Process. Technol. 177 (1) (2006) 621–625, http://dx.doi.org/10.1016/j.jmatprotec.2006.04.120.
[13] Q.V. Bui, J.-P. Ponthot, Numerical simulation of cold roll-forming processes, J. Mater. Process. Technol. 202 (1–3) (2008) 275–282, http://dx.doi.org/10.1016/j.jmatprotec.2007.08.073.
[14] R. Boman, J.-P. Ponthot, Continuous roll forming simulation using arbitrary Lagrangian Eulerian formalism, Key Eng. Mater. 473 (2011) 564–571, http://dx.doi.org/10.4028/www.scientific.net/KEM.473.564.
[15] A. Depauw, D. Herisson, R. Boman, R. Kergen, Roll forming of ultra high strength steels: progresses in experimental and modelling knowledge, in: Proceedings of International Roll Forming Congress 2009, Bilbao, Spain, 2009, pp. 101–108.
[16] J.-J. Sheu, Simulation and optimization of the cold roll-forming process, in: Materials Processing and Design: Modeling, Simulation and Applications-NUMIFORM 2004-Proceedings of the 8th International Conference on Numerical Methods in Industrial Forming Processes, vol. 712, AIP Publishing, 2004, pp. 452–457.
[17] M.O. Görtan, D. Vucic, P. Groche, H. Livatyali, Roll forming of branched profiles, J. Mater. Process. Technol. 209 (17) (2009) 5837–5844.

[18] L. Galdos, J. Larrañaga, L. Uncilla, H. Lete, G. Arrizabalaga, Process simulation and experimental tests of cold roll forming of a u-channel made of different ultra high strength steel, in: RollFORM'09: 1st International Congress on Roll Forming, Bilbao, Spain, 2009, pp. 75–82.
[19] J. Paralikas, K. Salonitis, G. Chryssolouris, Investigation of the roll forming flower design techniques on main redundant deformations on symmetrical profiles from AHSS, in: RollFORM'09: 1st International Congress on Roll Forming, Bilbao, Spain, 2009, pp. 83–91.
[20] J. Paralikas, K. Salonitis, G. Chryssolouris, Optimization of roll forming process parameters—a semi-empirical approach, Int. J. Adv. Manuf. Technol. 47 (9–12) (2010) 1041–1052.
[21] A. Abvabi, B. Rolfe, J. Larranaga, L. Glados, C. Yang, M. Weiss, Using the solid-shell element to model the roll forming of large radii profiles, in: Steel Research Journal: Proceedings of the 14th International Conference on Metal Forming, Wiley, 2012, pp. 711–714.
[22] J. Wiebenga, M. Weiss, B. Rolfe, A. Van Den Boogaard, Product defect compensation by robust optimization of a cold roll forming process, J. Mater. Process. Technol. 213 (6) (2013) 978–986.
[23] P. Groche, C. Mueller, T. Traub, K. Butterweck, Experimental and numerical determination of roll forming loads, Steel Res. Int. 85 (1) (2014) 112–122, http://dx.doi.org/10.1002/srin.201300190.
[24] data M Sheet Metal Solutions GmbH, COPRA FEA RF, http://www.datam.de/en/products-solutions/simulation-with-fea/.
[25] J. Chung, G.M. Hulbert, A time integration algorithm for structural dynamics with improved numerical dissipation: the generalized-α method, J. Appl. Mech. 60 (2) (1993) 371–375, http://dx.doi.org/10.1115/1.2900803.
[26] J. Donea, A. Huerta, J.-P. Ponthot, A. Rodríguez-Ferran, Arbitrary Lagrangian–Eulerian Methods, vol. 1, John Wiley & Sons, Ltd, 2004, pp. 413–437, Ch. 14.
[27] D.J. Benson, An efficient, accurate, simple ALE method for nonlinear finite element programs, Comput. Methods Appl. Mech. Eng. 72 (3) (1989) 305–350.
[28] R. Boman, J.-P. Ponthot, Efficient ALE mesh management for 3D quasi-Eulerian problems, Int. J. Numer. Methods Eng. 92 (10) (2012) 857–890, http://dx.doi.org/10.1002/nme.4361.
[29] R. Boman, J.-P. Ponthot, Finite element simulation of lubricated contact in rolling using the arbitrary Lagrangian–Eulerian formulation, Comput. Methods Appl. Mech. Eng. 193 (39) (2004) 4323–4353, http://dx.doi.org/10.1016/j.cma.2004.01.034.
[30] D.J. Benson, Momentum advection on unstructured staggered quadrilateral meshes, Int. J. Numer. Methods Eng. 75 (13) (2008) 1549–1580.
[31] R. Boman, J.-P. Ponthot, Enhanced ALE data transfer strategy for explicit and implicit thermomechanical simulations of high-speed processes, Int. J. Impact Eng. 53 (2013) 62–73, http://dx.doi.org/10.1016/j.ijimpeng.2012.08.007.
[32] J. Reinders, Intel Threading Building Blocks: Outfitting C++ for Multi-Core Processor Parallelism, O'Reilly Media, Inc., 2007.
[33] L. Dagum, R. Menon, OpenMP: an industry standard API for shared-memory programming, IEEE Comput. Sci. Eng. 5 (1) (1998) 46–55.
[34] A. Kuzmin, M. Luisier, O. Schenk, Fast methods for computing selected elements of the Green's function in massively parallel nanoelectronic device simulations, in: Euro-Par 2013 Parallel Processing, Springer, 2013, pp. 533–544.
[35] O. Schenk, K. Gärtner, Solving unsymmetric sparse systems of linear equations with PARDISO, Future Gener. Comput. Syst. 20 (3) (2004) 475–487.
[36] P. Flores, Development of experimental equipment and identification procedures for sheet metal constitutive laws, Ph.D. thesis, University of Liège, 2005.
[37] P. Flores, A.-M. Habraken, Material identification of dual phase steel DP1000, Tech. rep., University of Liège, 2005.
[38] Q.V. Bui, L. Papeleux, J.-P. Ponthot, Numerical simulation of springback using enhanced assumed strain elements, J. Mater. Process. Technol. 153 (2004) 314–318, http://dx.doi.org/10.1016/j.jmatprotec.2004.04.342.